Earth and Space Science

RESEARCH ARTICLE
10.1029/2023EA002883

The Paleozoic Hydrocarbon System in the Gotland Basin (Central Baltic Sea) Leaks

Arne Warwel[1,2], Christian Hübscher[1], Matthias Hartge[1], Maike Artschwager[3], Wiebke Schäfer[1,2], Jonas Preine[1], Tobias Häcker[1], Victoria Strehse[3], Jānis Karušs[4], and Thomas Lüdmann[3]

[1]Center for Earth System Research and Sustainability, Institute of Geophysics, University of Hamburg, Hamburg, Germany, [2]Now at GEOMAR Helmholtz Centre for Ocean Research Kiel, Kiel, Germany, [3]Center for Earth System Research and Sustainability, Institute of Geology, University of Hamburg, Hamburg, Germany, [4]Unit of Geology, University of Latvia, Riga, Latvia

Key Points:

- Numerous elongated fluid escape depressions are observed at the eastern margin of the Gotland Deep, central Baltic Sea
- First evidence for fluid migration pathways from Paleozoic toward Quaternary strata in the region
- Locations of fluid escape is controlled by the regional tectonic setting

Correspondence to:

C. Hübscher,
christian.huebscher@uni-hamburg.de

Citation:

Warwel, A., Hübscher, C., Hartge, M., Artschwager, M., Schäfer, W., Preine, J., et al. (2023). The Paleozoic hydrocarbon system in the Gotland Basin (central Baltic Sea) leaks. *Earth and Space Science*, *10*, e2023EA002883. https://doi.org/10.1029/2023EA002883

Received 14 FEB 2023
Accepted 22 MAY 2023

Author Contributions:

Conceptualization: Christian Hübscher, Jānis Karušs, Thomas Lüdmann
Data curation: Arne Warwel, Christian Hübscher, Matthias Hartge, Maike Artschwager, Wiebke Schäfer, Jonas Preine, Tobias Häcker, Victoria Strehse
Funding acquisition: Christian Hübscher
Investigation: Arne Warwel, Christian Hübscher, Matthias Hartge
Methodology: Arne Warwel, Matthias Hartge, Maike Artschwager, Wiebke Schäfer, Jonas Preine, Tobias Häcker, Victoria Strehse, Jānis Karušs, Thomas Lüdmann
Project Administration: Christian Hübscher, Thomas Lüdmann

Abstract The Baltic Basin is known for its numerous Paleozoic hydrocarbon reservoirs. There is published evidence that hydrocarbons are leaking from the seafloor, however, little is known about the hydrocarbon migration pathways from Paleozoic source and reservoir rocks toward the seafloor and their escape structures. To investigate these processes, we utilize a new set of multibeam, parametric sediment sub-bottom profiler and 2D seismic reflection data. The integrated analysis of seismic profiles, diffraction imaging and bathymetric maps allow to identify a hydrocarbon migration system within Silurian and Devonian strata that consists of layer parallel and updip migration beneath sealing layers, migration across seals along faults, and seafloor escape structures in form of elongated depressions. The general migration trend is directed updip, from the Paleozoic reservoirs below the southeastern Baltic Sea toward the Gotland Depression in the northwest. The locations of the hydrocarbon escape structures at the seafloor and their elongated shape are mainly controlled by the regional geological setting of outcropping Paleozoic layers. In addition, iceberg scouring may have facilitated hydrocarbon migration through the Quaternary deposits. The description of this hydrocarbon migration system fills the gap between the known reservoirs and the observed hydrocarbon accumulations and seepages. With regard to potential Carbon Capture and Storage projects, the identification of this hydrocarbon migration system is of great importance, as potential storage sites may be leaking.

Plain Language Summary The Baltic Basin including the Baltic Sea is well known for its hydrocarbon reservoirs with ongoing oil production since the 1940s. While there is some published evidence that hydrocarbons are leaking from the seafloor, little is known about the pathways from the reservoirs toward theses leakages. In this study, we use three imaging techniques for the seafloor, the uppermost sediments and the first few kilometers of the subsurface to image the hydrocarbon migration pathways and their escape structures. We find that hydrocarbons are migrating along dipped geological layers from the reservoirs in the southeast toward the Gotland Deep in the northwest. Additionally, we also observe that hydrocarbons are penetrating through these geological layers at locations of pre-existing small-scale fractures. The locations, at which the hydrocarbons escape from the seafloor, are mainly controlled by the regional tectonic setting. In addition, iceberg scouring may have had an influence on the exact escape locations. With our findings in this study, we fill the gap between the known reservoirs and the observed seepages and can contribute to questions regarding the potential storage of CO_2 in the Baltic Basin.

1. Introduction

Hydrocarbons leaking from the seafloor into the oceans affect the shallow seafloor biosphere and the water column and thus can contribute to the pollution of the oceans (Dewar et al., 2013; Judd, 2003; Judd & Hovland, 2009; MacDonald et al., 2002; Mityagina & Lavrova, 2016). However, they also represent a kind of window through which geological and geochemical processes as well as geological structures in the Earth's crust can be studied (Heggland, 1998; Hovland et al., 2002; Römer et al., 2021). Utilizing these aspects can contribute to a better understanding of subsurface processes and structures and, therefore, also aid to understanding the economic potential of the subsurface. In particular, hydrocarbon migration pathways through the subsurface and hydrocarbon sealing layers play an important role in the exploration of suitable sites for Carbon Capture and Storage (CCS)

Software: Arne Warwel, Matthias Hartge, Maike Artschwager, Wiebke Schäfer, Jonas Preine, Tobias Häcker, Victoria Strehse
Supervision: Christian Hübscher
Visualization: Arne Warwel
Writing – original draft: Arne Warwel
Writing – review & editing: Arne Warwel, Christian Hübscher, Wiebke Schäfer, Jonas Preine, Victoria Strehse, Thomas Lüdmann

or the storage of nuclear waste and hydrogen (Shogenov et al., 2017; Shogenova et al., 2009; Tarkowski, 2017). A detailed knowledge of these pathways and sealings is therefore of outstanding importance.

The Baltic Basin located in northeastern Europe is well-known for the occurrence of hydrocarbons. Oil production on the island of Gotland has been ongoing since the 1940s (Johansson et al., 1943). Within the Gotland Depression (Figure 1a), the outflow of hydrocarbons has been documented in several instances. Flodén et al. (2001) described clear indications for hydrocarbon seepages in Silurian reef systems east of Gotland, which can be seen as oil stains on the water surface on calm days. Wagner (2011) mapped a zone of increased hydrocarbon concentration, both in bottom sediments and bottom water within the Polish territorial waters of the southern Baltic Sea. These authors attributed the main fluid migration routes of liquid and gaseous hydrocarbons originating from subsurface geological structures to major fault zones and related systems of fissures. However, they also discussed the migration of subsurface hydrocarbons through the pinch-out zones of sedimentary complexes. Endler (1998) observed individual pockmarks at the shoulders of the Gotland Deep and Schäfer et al. (2021) showed that the Klints Bank (Figure 1a), a giant drumlin, seals hydrocarbon fluids and suggested that they originate from reservoirs located beneath Latvia. Even though a northwestward migration of hydrocarbons along sealing reflectors within the Baltic Basin has been suggested (Schäfer et al., 2021; Sivhed et al., 2004), a comprehensive analysis and evidence of such a migration system is yet missing. In addition, the escape paths and structures of the fluids through the seafloor are also largely underexplored in vast parts of the central Baltic Basin.

The potential of the central Baltic Basin region for CCS has been of interest for several years (O'Neill et al., 2014; SLR Report, 2014; and references therein). The BASTOR project identified and characterized potential CO_2 storage sites in the southern Baltic. Several saline aquifer closures within Cambrian sandstones that group along the fault systems of the Liepaja-Saldus Ridge (Figure 1b) were regarded as especially suitable (SLR Report, 2014). Within the Swedish sector, Sopher et al. (2014) considered Middle Cambrian Faludden sandstones as the most promising storage potential.

In this study, we utilize high-resolution seismic, sub-bottom profiler and multibeam echosounder data from the Baltic Depression within the exclusive economic zones of Estonia, Latvia and Lithuania. The data were collected in fall 2021 during the RV METEOR expedition M177 (Hübscher et al., 2022). We strive to test the hypotheses from Sivhed et al. (2004) and Schäfer et al. (2021) that hydrocarbons migrate from the known reservoirs in the southeastern Baltic Sea along dipped and sealing rock layers into the Baltic Depression. Additionally, we aim to identify possible seafloor fluid escape structures and to delineate the origin of the expelling fluids from shallow biogenic gas formed in post-glacial sediments. The identification of potential hydrocarbon migration pathways and seepages can then be used in future considerations regarding the potential of CCS or other storage-related aspects in the central Baltic Basin.

2. The Baltic Basin

The sedimentary Baltic Basin is a NE-SW trending epicontinental basin, which is centered below the southern Baltic Sea overlaying the eastern margin of the East European Craton (Šliaupa & Hoth, 2011; Ziegler, 1990). It includes parts of Sweden, Poland, Latvia, Lithuania and Estonia (Figure 1b) (Sopher et al., 2016; Ziegler, 1990). To the southeast, the Baltic Basin is bounded by the Mazury-Belarus High separating it from the Lublin-Podlasie Basin, while further to the southwest and west it terminates against the Teisseyre-Tornquist Zone and the Sorgenfrei-Tornquist Zone disconnecting it from the Polish Trough, the North German Basin and the Danish Basin (De Vos et al., 2010; Šliaupa & Hoth, 2011). In the north and northwest, the Baltic Basin extends up to the southeastern border of the Fennoscandian Shield (Figure 1b) (Šliaupa et al., 2006). The thickness of the sedimentary record varies considerately between less than 100 m in northern Estonia, between 1,900 and 2,300 m in Latvia and Lithuania and more than 4,000 m in Poland (Šliaupa & Hoth, 2011). The strata are tilted to the SE, creating a sequence of Lower Paleozoic layers that outcrop beneath Quaternary deposits. The basin is crossed by a system of faults and uplifted basement blocks that constitute the Liepaja-Saldus Ridge (Figure 1b). This ridge is over 700 km long, oriented in the NE-SW direction and located in the Latvian part of the Baltic Sea as well as the Latvian mainland (SLR Report, 2014; Tuuling, 2019). At its western end, it is bounded by the Leba Ridge, which is a similar system of fault zones that is oriented in the N-S direction and extends from the central Baltic Basin toward Poland (Figure 1b) (Tuuling, 2019).

2.1. Geological Evolution

The evolution of the Baltic Basin began during Late Ediacaran to Early Cambrian times and can be related to the break-apart of the Rodinia supercontinent and an associated extensional tectonic regime (Šliaupa et al., 2006;

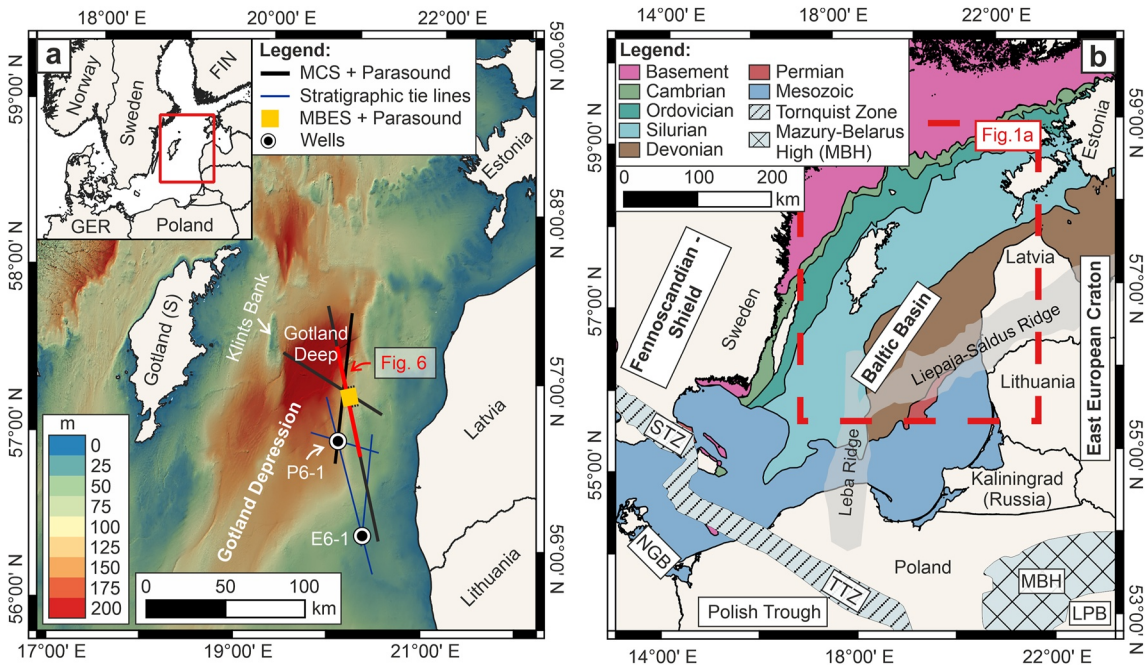

Figure 1. (a) Bathymetric map of the central Baltic Basin including the Gotland Depression and the Gotland Deep (EMODnet, 2020). Symbols indicate seismic and sub-bottom profiler lines, multibeam surveys and wells used in this study. A detailed map of the MBES survey and the seismic lines in that area is shown in Figure 3. (b) Overview of the marine bedrock geology within the Baltic Basin and major geological structures of the Baltic region. Compiled after Grad and Polkowski (2016), Mazur et al. (2015), Šliaupa et al. (2006), Sopher et al. (2016), and Tuuling (2019). MCS: Multi-Channel Seismic; MBES: Multibeam Echosounder; STZ: Sorgenfrei-Tornquist Zone; TTZ: Teisseyre-Tornquist Zone; MBH: Mazury-Belarus High; NGB: North German Basin; LPB: Lublin-Podlasie Basin.

Šliaupa & Hoth, 2011). Lithospheric extension, as well as sedimentary and thermal loads, initiated a long-lasting period of subsidence affecting the passive continental margin basin. The basin deepening ceased during the Cambrian and the Baltic Basin was flooded during a basin wide marine transgression. The following Ordovician is characterized by a shallow marine environment and continuous sedimentation (Šliaupa & Hoth, 2011). Missing evidence of significant faulting during the Cambrian, Ordovician and Early Silurian suggest a low level of tectonic stresses affecting the Baltic Basin during these times. The only observed fractures are located offshore Latvia and Lithuania with fault throws of only a few dozen of meters. This faulting has been related to compressional tectonic activity due to East Avalonia docking during the Late Ordovician (Šliaupa & Hoth, 2011). The collision with East Avalonia also caused an increased rate of subsidence, which continued during the Silurian (Poprawa et al., 1999).

The next main phase of basin formation and structural development of the Baltic Basin took place in the latest Silurian and earliest Devonian during the Caledonian Orogeny and the collision of Laurentia and Baltica (Šliaupa, 1999). Many structures formed during this period, including deep rooted structures such as the Liepaja-Saldus Ridge and Leba Ridge, still outline the present-day morphology of the Baltic Sea region (Gelumbauskaitė, 1995; Tuuling, 2019; Šliaupa et al., 2006). The Baltic Basin developed as a flexural foreland basin creating a significant accommodation space, where thick sequences of Silurian and Devonian sediments were deposited under marine and increasingly shallow marine, lagoonal and deltaic conditions (Tuuling et al., 2011; Šliaupa et al., 2006; Šliaupa & Hoth, 2011). Silurian deposits are characterized by carbonaceous clays, dolomitic and limey marls, clayey limestones and dolomites with a high content of fossil faunas, while Devonian layers mainly consist of various forms of clays, sandstones and dolomites (Usaityte, 2000). The persisting basin subsidence ceased due to tectonic activity related to the Variscan orogeny during the early Carboniferous, initiating a phase of non-deposition, uplift and erosion. Consequently, Carboniferous and Permian sections are missing in large parts across the Baltic Basin (Tuuling et al., 2011; Šliaupa & Hoth, 2011). Thermal relaxation re-established a regime of subsidence during the Late Permian, however, only episodic sedimentation related to marine transgressions caused by global sea level changes occurred during the Mesozoic and Cenozoic (Šliaupa & Hoth, 2011). Throughout large parts of the Mesozoic, the Baltic Basin was affected by only minor tectonic activity. In the south westernmost part, this changed in the Late Cretaceous with the establishment of strike-slip and

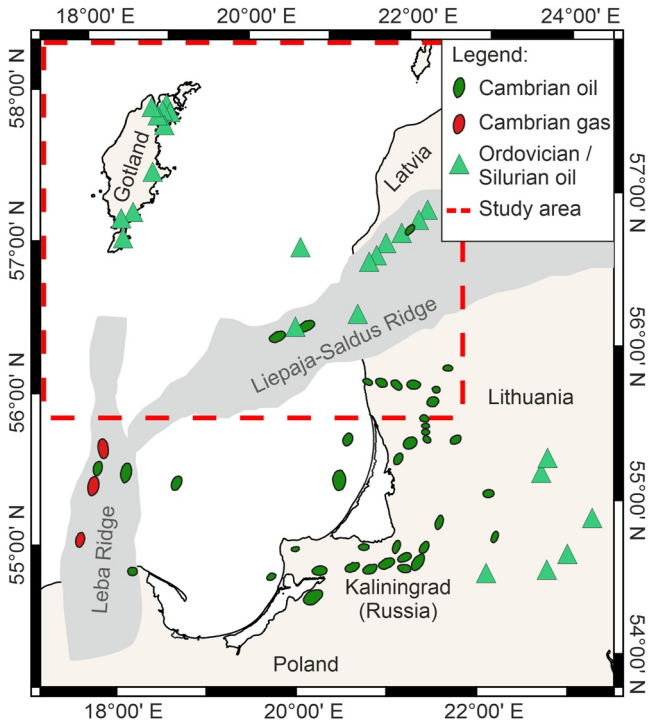

Figure 2. Locations of oil and gas discoveries in Lower Paleozoic successions in the Baltic Basin (compiled after Brangulis et al. (1992), Kanev et al. (1994), and Šliaupa and Hoth (2011)).

reverse faults. The Sorgenfrei-Tornquist Zone was uplifted by up to 2,000 m during the Late Cretaceous inversion phase and the regional uplift of Fennoscandia during the Neogene (Šliaupa & Hoth, 2011). Uplift of Fennoscandia during the Miocene also caused tilting of the backslope in eastern Sweden and toward the Baltic Basin (Hall & van Boeckel, 2020; Lidmar-Bergström & Olvmo, 2015).

The Quaternary history of the Baltic Basin is characterized by the influence of several phases of glaciation during the Pleistocene. During at least three glaciation periods, the Elsterian, the Saalian and the Weichselian glaciations, the Baltic Basin was fully covered by ice sheets (e.g., Ehlers et al., 2011; Houmark-Nielsen, 2011; Huuse & Lykke-Andersen, 2000). The direction of the main ice flow was thereby south-southwestward approximately parallel to Sweden's present-day shoreline (Hall & van Boeckel, 2020; Woźniak & Czubla, 2015). Intensive glacial erosion removed large parts of the Quaternary and underlying Paleozoic successions (Šliaupa & Hoth, 2011). Following the end of the last glacial maximum (Weichselian glacial) about 10,000 years ago, the present-day Baltic Sea evolved (Andrén et al., 2011). The causes for the formation of the Gotland Depression including the Gotland Deep in the central Baltic Basin (Figure 1a) are still not fully understood, especially regarding the role of tectonic and erosional processes (Šliaupa & Hoth, 2011). Gelumbauskaitė (1995) linked the formation of the Gotland Deep east of Gotland to the interaction of tectonic and eustatic processes as well as denudation and glacioisostasy in context of the latest glacial periods. The author also noted that its development was closely related to the evolution of the Fennoscandian Shield, as the base of the Gotland Deep originates on the former peneplain of the Fennoscandian Shield. The Gotland Deep reaches the greatest water depths of up to 250 m in the region (Figure 1a). To its west, it is bounded by a morphologic high, the Klints Bank (Figure 1a). In a recent study, Schäfer et al. (2021) showed that the Klints Bank is of glacial origin and suggested that it is an extraordinarily large submarine drumlin.

2.2. Hydrocarbons in the Baltic Basin

The Baltic Basin hosts a vast amount of hydrocarbon source rocks and reservoirs. More than 700 deep wells have been drilled and more than 40 accumulations of hydrocarbons have been discovered (Dobrova et al., 2003; Šliaupa et al., 2004; Šliaupa & Hoth, 2011; Zdanaviciute & Lazauskiene, 2004). Occurrences are known from Sweden, Estonia, Latvia, Lithuania, Poland and the Kaliningrad District of Russia (Zdanaviciute & Lazauskiene, 2004). Figure 2 summarizes the locations of oil and gas discoveries in the Baltic Basin. Although most of the discovered hydrocarbons are oil accumulations, some gas accumulations are also reported from offshore Poland (Šliaupa & Hoth, 2011). The main reservoirs for hydrocarbons in the Baltic Basin are Middle and Upper Cambrian sandstone layers, which are sourced by organic-rich late Cambrian to Tremadocian black shales (Alum Shale) and upwards sealed by Ordovician and Silurian shales (De Vos et al., 2010; Pletsch et al., 2010). The total thickness of these sandstone reservoirs is comparably small and varies between 50 and 70 m with a thickness reduction toward the east (De Vos et al., 2010; Šliaupa & Hoth, 2011). Particularly rich Cambrian reservoirs were identified within the Liepaja-Saldus and Leba Ridges with average porosities between 14% and 18% (Šliaupa & Hoth, 2011). In the northern and northeastern part of the Baltic Basin, Ordovician carbonate layers represent additional hydrocarbon reservoirs, even though they are volumetrically less significant than the Cambrian reservoirs (De Vos et al., 2010). Although their reservoir properties are generally poor (e.g., low porosity), oil accumulations have been reported from the Liepaja-Saldus Ridge area in western Latvia (Figure 2) (Šliaupa & Hoth, 2011). Oil production from Upper Ordovician carbonate mounts on the island of Gotland has been ongoing since the 1940s with a total oil production of 100,000 m^3 between 1974 and 1992 (Johansson et al., 1943; Sivhed et al., 2004). Furthermore, Flodén et al. (2001) described clear indications for hydrocarbon seepages above Lower and Upper Silurian reefs east of Gotland. Other studies, however, could not verify the presence of hydrocarbon accumulations within these reef structures (Šliaupa & Hoth, 2011). As Upper Ordovician Caradocian and Lower Silurian Llandoverian shales are principally thermally mature enough to generate hydrocarbons and several oil accumulations

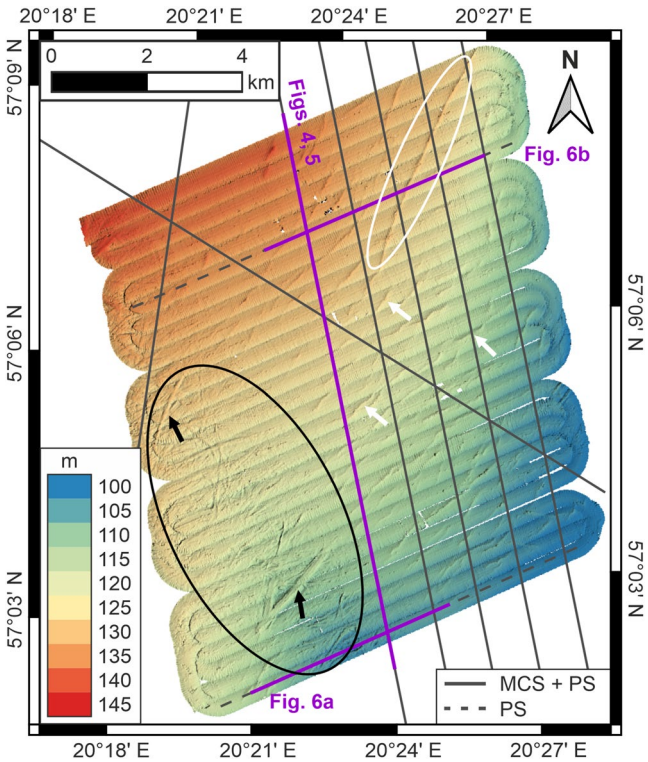

Figure 3. High-resolution bathymetric map covering the area at the eastern margin of the Gotland Deep (for location see Figure 1a). White arrows denote three exemplary NE-SW oriented, channel-like structures incising into the seafloor. The white ellipse emphasizes such a structure that is extraordinarily long. The black ellipse highlights an area where the seafloor is characterized by a rough and scraped-like surface, while the black arrows denote NE-SW-oriented channels within this area. MCS: Multi-Channel Seismic; PS: PARASOUND (sub-bottom profiler).

were discovered within Upper Silurian reefs in central Lithuania, the Silurian reef structures east of Gotland still represent potential hydrocarbon reservoirs (De Vos et al., 2010; Lapinskas, 2000; Šliaupa & Hoth, 2011). A major regional sealing structure for different hydrocarbon accumulations in the Lower Paleozoic strata within the Baltic Basin is the Upper Silurian sedimentary succession, which mainly consist of shales, mudstones and marls with thicknesses of up to a few thousand meters (De Vos et al., 2010).

Wagner (2011) observed and mapped a zone of increased hydrocarbon concentration related to oil spills in shallow sediments and bottom water along tectonic faults of the Teisseyre-Tornquist Zone offshore Poland. The author associated the observed oil with Middle Cambrian oil reservoirs. The migration paths of these fluids are assumed to be connected to major fault zones and related systems of fissures. However, the author also found evidence for hydrocarbon migration paths related to pinch-outs of particular stratigraphic layers. Sivhed et al. (2004) proposed that the hydrocarbons migrate updip along stratigraphic horizons from the central parts of the Baltic Basin toward Gotland. A similar assumption was made by Schäfer et al. (2021), who observed hydrocarbon accumulations underneath the Quaternary units of the Klints Bank. They suggested that these accumulations must have migrated there and based on the tectonic setting also assumed an updip migration from the southeast toward the northwest. Endler (1998) observed indications for dispersed gas in the uppermost sediments at the northwestern flank of the Gotland Deep and some individual pockmark structures at its southwestern flank. Based on the location of the observed pockmarks above an uplifted block structure, the author assumed a thermogenic origin for these pockmarks located in the sedimentary bedrock. For the gassy sediments, the author favored a biogenic origin, as the dispersed gas concentrates in the uppermost layers only. Endler (1998) also noted that there are no indications for hydrocarbons occurring in the sediments of the central Gotland Deep.

3. Data and Methods

Our database mainly consists of geophysical data acquired during the RV METEOR expedition M177 in October/November 2021 (Figures 1 and 3) (Hübscher et al., 2022). During this expedition, more than 4.600 km of seismic and sediment sub-bottom profiler data as well as approximately 1,590 km^2 of multibeam echosounder (MBES) data were acquired in the central Baltic Basin. In this study, we analyze a sub-set from the southeastern margin of the Gotland Deep (Figures 1a and 3). Besides the M177 data, we make use of some additional seismic profiles acquired during the RV ALKOR expedition AL515 in September 2018 that are located in the vicinity of our study area. The locations of the used datasets are depicted in Figures 1a and 3.

All seismic profiles were acquired using a 144-channel digital streamer with an active length of 600 m towed about 100 m behind the ship's stern. The seismic source consisted of one or two (AL515/M177) GI-Pulser firing approximately every 10/4.7 s (AL515/M177), resulting in a nominal shot interval of about 26/13 m (AL515/M177). Seismic data processing was performed using the 2021 VISTA SEISMIC DATA PROCESSING software by Schlumberger and divided into pre-processing, multiple attenuation and post-stack processing. Pre-processing consisted of geometry-setup, filtering, despiking and spherical gaining. For multiple attenuation, we applied a predictive deconvolution in the τ-p domain, surface related multiple attenuation (SRME) (Verschuur et al., 1992) and an f-k filtering attenuation scheme based on move-out differences between primary and multiple reflections (Yilmaz, 2001). In between these steps we performed several iterations of manual velocity analysis. The post-stack processing included migration, white noise suppression (4D-DEC), time-variant filtering and RMS scaling. The vertical resolution of the final seismic images calculated with a velocity of 2,000 m/s is about 5 m.

The seismic profiles are linked to the Latvian offshore wells E6-1 and P6-1 by means of seismic tie lines from the AL515 data set (blue lines in Figure 1a). This provides a stratigraphic tie enabling a stratigraphy-based

interpretation. Stratigraphic correlation and subsequent interpretation were performed using the 2019 KINGDOM software by IHS Markit. Further interpretation was conducted by calculating and analyzing the seismic instantaneous frequency attribute, which is considered a direct hydrocarbon indicator (Taner et al., 1979). Low instantaneous frequencies or low-frequency shadows are considered as an indicator for the presence of hydrocarbons (Abu El-Ata et al., 2019; Tai et al., 2009; Taner et al., 1979).

In addition to the conventional seismic data processing, we performed dedicated diffraction imaging for selected seismic profiles in order to enhance the visibility of faults and fractures. As diffractions occur when the seismic wavefield is radially scattered at an abrupt heterogeneity that is comparable in size with the dominant wavelength or even below, they carry valuable information about for example, faults, pinch-outs and irregular erosional surfaces (e.g., Kearey et al., 2002; Landa & Keydar, 1998; Schwarz, 2019a). The imaging technique consists of two stages, which are given by the separation of the weak diffracted wavefield from the usually stronger reflected wavefield and the subsequent diffraction focusing and imaging. The diffraction separation follows the coherent separation approach introduced by Schwarz and Gajewski (2017) and extended by Schwarz (2019b), in which the reflected wavefield is estimated through coherent wavefield summation and then subtracted from the full recorded wavefield to arrive at a reflection-free diffraction field. In the second step, this diffraction field is focused using Finite Difference migration. The squared envelope of the focused diffraction field is referred to as diffraction energy and blended with the conventionally processed and time-migrated seismic image to provide the final image (cf. Preine et al., 2020). The joint display of the full-wavefield image and the diffraction energy as an additional seismic attribute enables the identification of even small-scale faults and fractures and facilitates their interpretation (Ahlrichs et al., 2023; Preine et al., 2020).

For the parametric sub-bottom profiler surveys, we used the hull-mounted transducer of the PARASOUND system that emits a 4 kHz signal that penetrated the first several tens of meters below the seafloor. The data were digitized and stored in SEG-Y format. Processing included geometry setup and bandpass filtering. Further analysis and stratigraphic interpretation were performed using the 2021 PETREL software by Schlumberger. The stratigraphic interpretation is based on a nearby sediment core (Christiansen et al., 2002) and the comparison of characteristic properties (e.g., amplitude, reflection pattern) with other publications (e.g., Endler, 1998; Winterhalter, 2001; Zecchin & Rebesco, 2018).

The high-resolution bathymetry was acquired using the hull-mounted Kongsberg EM710 multibeam swath sounder system, which operates in a frequency range between 70 and 100 kHz. The data were calibrated with the water velocity by using two sound velocity measurements. For manual processing of data errors and gridding with a grid size of 5×5 m, we utilized the QPS QIMERA software. Due to bad weather during the acquisition and the resulting ship movements, some errors and artifacts (e.g., periodic wobbling) remained in the data even after intensive processing (Hübscher et al., 2022).

4. Results

4.1. Seafloor Morphology

The bathymetric map displayed in Figure 3 is located at the eastern margin of the Gotland Deep (see Figure 1a) and images the local seafloor morphology of this area. The seafloor gently dips northwestwards with an angle of about 0.2° from water depths of less than 100 m in the southeast toward water depths of about 140 m in the northwest. With the exception of the western and southwestern parts, it depicts a generally smooth surface that is disrupted by scattered incisions of varying shapes and sizes. Especially the central and eastern parts are dominated by NE-SW oriented, elongated and channel-like incisions in the seafloor. Their lengths vary mostly in the range of a few hundred meters, their widths are usually less than 50–100 m and their depths vary between 1 and 3 m. The paths of these structures are mostly straight with only minor bending or curvatures and the individual structures are not connected to each other. Three examples of these structures are denoted by white arrows in Figure 3. In the northeast of the mapped area, there is an incising structure whose length exceeds 5 km, while its width and depth are similar to the other structures (white ellipse in Figure 3).

In the west and especially the southwest, the bathymetric map shows a fundamental change in the seafloor morphology. The seafloor is rough, irregular and exhibits scraped-like features that are both incising and pinching out of the seafloor. These structures are chaotic and not oriented in a favored direction. In contrast to the previously described structures in the central and eastern parts, they are positioned closer together and also tend to

cross and overlap each other. A particularly striking area containing these structures is marked by a black ellipse in Figure 3. The pattern of the rough and chaotic structures in the west and southwest is interrupted by two distinct channel-like features that are wider and deeper than the chaotic structures (black arrows in Figure 3). They are oriented in the NE-SW direction and overprint some of the other structures.

4.2. Paleozoic and Quaternary Successions

The seismic image illustrated in Figure 4a crosses the bathymetric map shown in Figure 3 in NW-SE direction and extends further toward the Gotland Deep in the northwest and the Liepaja-Saldus Ridge in the southeast (see Figures 1a and 3). The area of the multibeam survey is marked at the eastern margin of the Gotland Deep. Figure 4b shows the stratigraphic interpretation of this seismic section based on the E6-1 and P6-1 wells. The Paleozoic successions consist of Cambrian, Ordovician, Silurian and Devonian strata, which are all heavily tilted toward the southeast. Silurian and Devonian deposits truncate unconformably against the base of the Quaternary strata. In the lower part of the Silurian succession until the Mid-Silurian carbonate reflection (see Sopher et al., 2016), we observe sub-parallel and sometimes divergent reflection packages with low to medium amplitudes. Starting at a distance of approximately 20 km, these reflection packages are superimposed by chaotic noise, which represents residual multiple energy that could not be removed during the multiple suppression processing. At a distance of about 25 km, the Mid-Silurian carbonate reflection exhibits an irregular, upwards bent-like shape that is terminated by a small fracture in the southeast (Figure 4a). The location of this structure correlates with Silurian reefs mapped and described by Flodén et al. (2001). In the upper part of the Silurian succession, the internal reflection pattern is mostly sub-parallel with medium to high amplitudes. Especially at distances between 30 and 40 km, the sub-parallel reflections are disrupted by small-scale, almost vertical fractures with a vertical displacement of just a few milliseconds (light green in Figure 4a). The top Silurian/base Devonian reflection deviates from the characteristics of the internal upper Silurian reflections. It is blurred, much wider than the other reflections and gives the impression of much lower frequency content. The displayed Devonian successions are mostly low to medium amplitude interrupted by a sub-parallel/wavy-parallel reflection package with high amplitudes that could represent the transition from the Middle to Lower Devonian. Except for this prominent reflection package, the internal reflection pattern is partly sub-parallel and partly transparent/blanked so that no distinct pattern can be identified.

The locations of the small-scale fractures observed within the Upper Silurian reflection package (Figure 4a) were further investigated by diffraction imaging. Figure 4c displays the seismic reflection image overlain with the corresponding diffraction energy (c.f. Ford et al., 2021; Preine et al., 2020; Schwarz & Krawczyk, 2020). Red colors in the diffraction image indicate high diffractivity values, thus indicating the presence of diffraction-generating features. High diffractivity values are especially visible at the base Quaternary reflection package. Other areas with increased diffractivity can be recognized around the Silurian reef structure and at the observed small-scale fractures. At those fractures, the diffraction energy vertically aligns with the offset between the reflectors and thus traces the fault plane. It becomes visible that small fractures are lining up next to each other, whereby the displacements caused by these fractures between the individual reflections are always only a few milliseconds.

The Quaternary deposits in the seismic image shown in Figures 4a and 4b exhibit varying thicknesses and characteristics. Within the Gotland Deep in the northwest, the deposits are about 0.05 s TWT (40 m) thick, well layered and of post-glacial origin. At the flank of the Gotland Deep and in the area of the multibeam survey, the thickness reduces to a minimum thickness of about 0.025 s TWT (20 m). Below the high amplitude seafloor reflection, the Quaternary deposits are not well resolved. Only the presence of thin reflection inlays hint toward the existence of thinner layers that are below the seismic resolution. Further toward the southeast, the thickness increases and reaches a maximum thickness of about 0.1 s TWT (80 m). To the southeast of the multibeam survey, several irregular peaks are pinching out at the seafloor. The reflection pattern underneath is chaotic with medium amplitudes. Bounded by this area is a valley-like structure, which infill is hummocky/sub-parallel layered and shows medium amplitudes. In the southeast, the valley is bounded by chaotic deposits, where the amplitude changes from high at the seafloor to medium/low at the base Quaternary.

The Quaternary successions within the area of the multibeam survey (Figure 3) are further investigated by three sub-bottom profiler images shown in Figures 5 and 6. Identical to Figure 4, the profile illustrated in Figure 5 crosses the bathymetric map in the NW-SE direction (Figure 3). The acoustic basement is mostly transparent and comprises the pre-glacial Paleozoic successions. The basement is overlain by a layer, which is opaque in

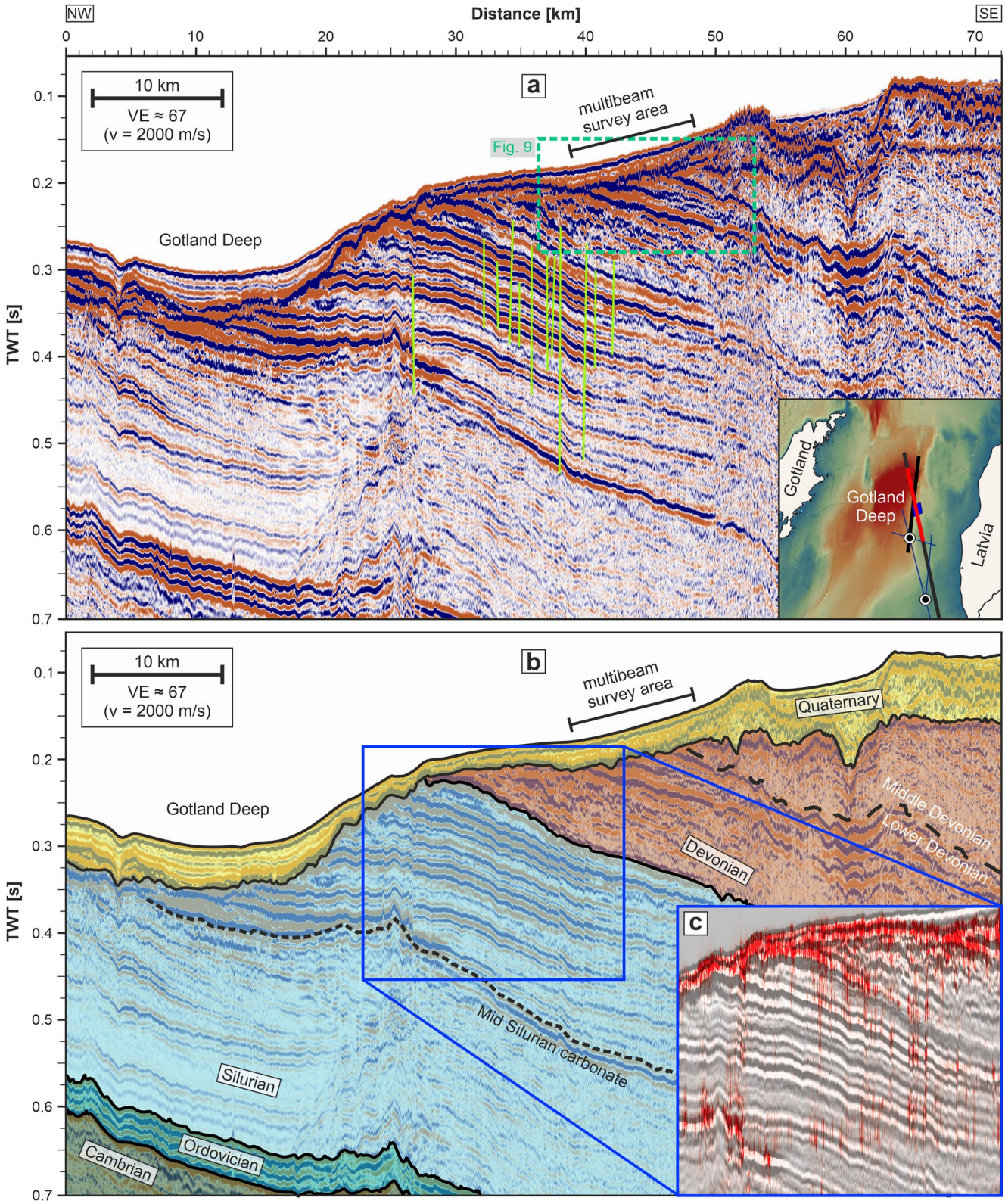

Figure 4. (a) Seismic image crossing the multibeam survey area and reaching into the Gotland Deep. Light green lines indicate small fractures and faults. (b) Stratigraphic interpretation of (a). (c) Diffraction energy image for the small-scale fractures marked in (a) (red color indicates high diffraction energy). For location of the profile see the red line in the inset map in (a).

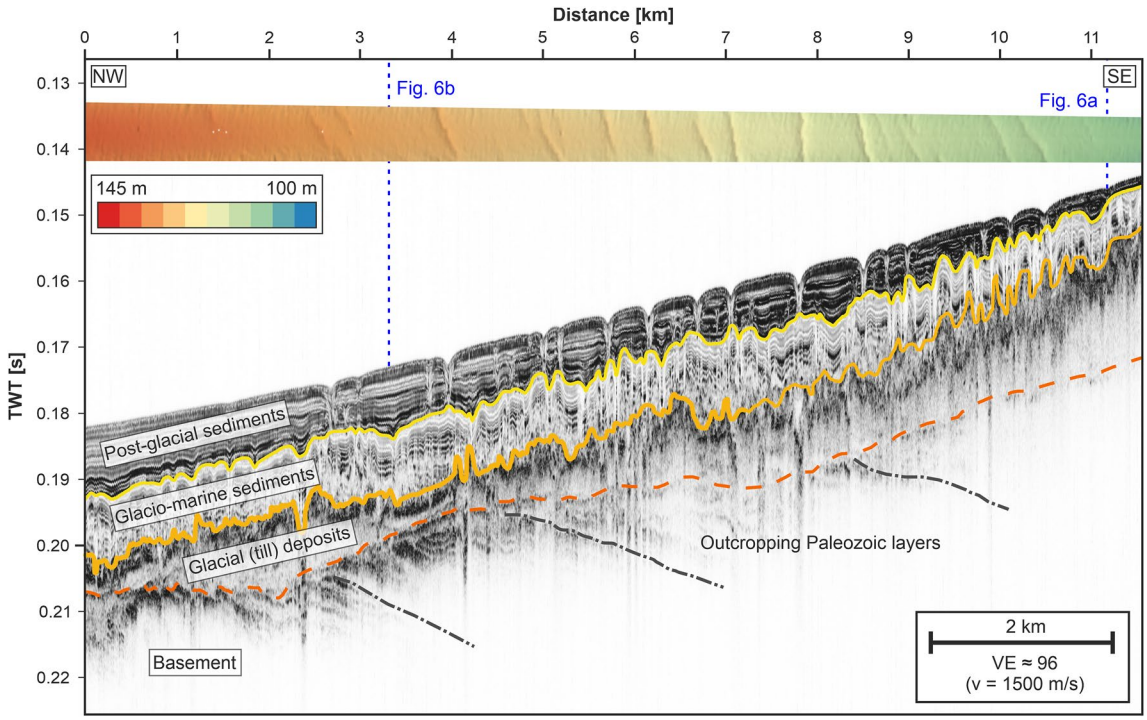

Figure 5. Sub-bottom profiler image crossing the multibeam survey area from north to south showing three different layers of Quaternary deposits. The colored image at the top shows the corresponding multibeam echosounder data. For location, see Figure 3.

the lower part and becomes higher in amplitude, chaotic and irregular in the upper part. These characteristics are common for subglacial till deposits (e.g., Endler, 1998; Winterhalter, 2001; Zecchin & Rebesco, 2018). Assembled on top of the till deposits is a layer characterized by undulating low to high amplitude reflections that are mostly parallel/wavy-parallel, partly continuous and laminated. Continuous sections of these reflection packages are disrupted by areas where the underlying till deposits create an especially rough surface. The internal shape and structure of this layer indicates that it depicts glaciomarine sediments deposited under a combination of glacial- and marine-related processes (Endler, 1998; Licht, 2009; Zecchin & Rebesco, 2018). The uppermost layer consists of medium to high amplitude, mostly continuous and parallel/wavy-parallel layered reflections. Irregularities at the base of the layer are leveled toward the layer top. A nearby sedimentary core dates this unit to post-glacial Holocene sediments deposited under marine conditions (Christiansen et al., 2002). Striking for this

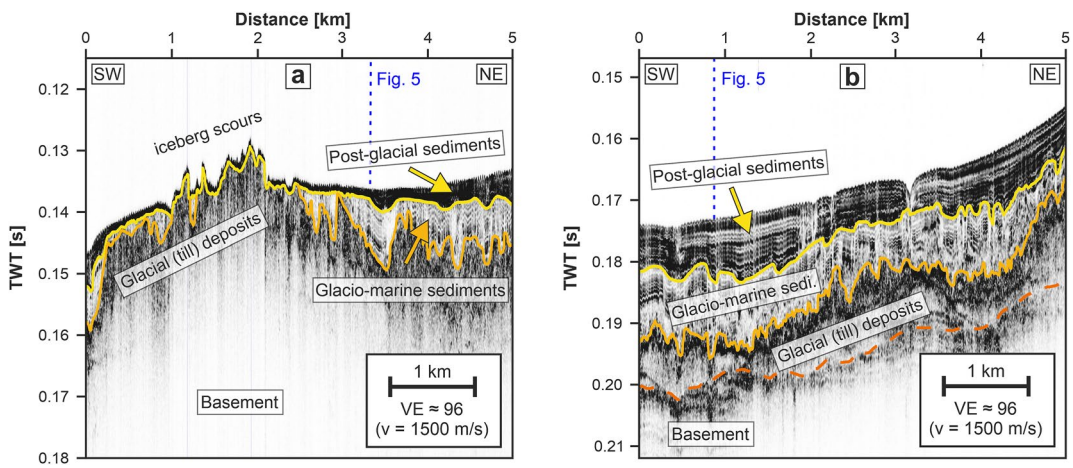

Figure 6. Sub-bottom profiler images crossing the chaotic structures observed in the southwest of the bathymetric map (a) and the extraordinary long incisions in the northeast (b). For location, see Figure 3.

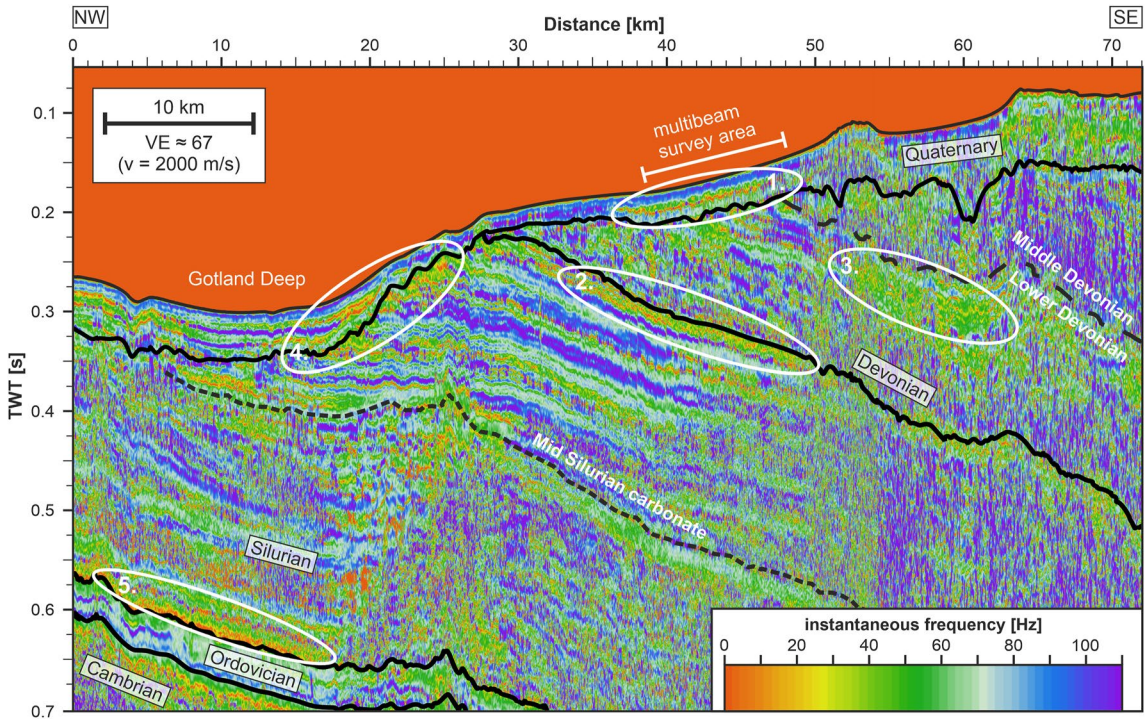

Figure 7. Instantaneous frequency plot calculated for the seismic image shown in Figure 4a.

layer are several channel-like incisions at the seafloor. Almost transparent areas below these structures extend into the glaciomarine sediment layer and disrupt the otherwise continuous reflection patterns. The incisions are also visible in the bathymetry recorded along this profile that is displayed on top of the sub-bottom profiler image in Figure 5.

Figure 6 illustrates two sub-bottom profiler images that are orientated perpendicular to the one shown in Figure 5. Figure 6a crosses the chaotic, scrape-like structures observed in the southwest of the mapped bathymetry, while Figure 6b crosses the extraordinarily long incision observed in the northeast (Figure 3). Similar to Figure 5, we observe three layers consisting of glacial till deposits, glaciomarine sediments and post-glacial Holocene sediments. In Figure 6a, the glacial till deposits exhibit a rough and irregular surface with several distinct peaks. Within that profile between distances of 1 and 2 km, the seafloor is shaped by these till deposits, which in this area are only overlain by a thin layer of post-glacial sediments. Toward the northeast, the thickness of the post-glacial sediments increases. Glacio-marine sediments are only present in the northeast and southwest away from the area, where the till layer shapes the seafloor. The characteristics of the Quaternary layers shown in Figure 6b are very similar to the ones in Figure 5. The extraordinarily long channel-like structure observed in the bathymetry (white ellipse in Figure 3) is clearly visible at a distance of about 3 km. The shape of this structure and the almost transparent area below it corresponds to the observations made in Figure 5.

4.3. Hydrocarbon Indicators

An instantaneous frequency plot of the seismic image depicted in Figure 4a is shown in Figure 7. Low frequencies, which can act as direct hydrocarbon indicators, are displayed in red/yellowish, while high frequencies are displayed in blue/purple. Several areas marked in Figure 7 with white ellipses within the Silurian, Devonian and Quaternary successions are particularly striking. Area 1 correlates with the location of the multibeam survey at the margin southeast of the Gotland Deep. Low frequencies are observed within the lower and middle parts of the Quaternary deposits at this location. Area 2 is located at the border between Silurian and Devonian between approximately 30 and 50 km. Here, low frequencies are visible right below the base Devonian. This area of low frequencies corresponds to the blurred reflector observed at this location in Figure 4a. While the low frequencies below the base Devonian represent an elongated but narrow band, low frequencies within area 3 located at the

transition of Lower to Middle Devonian are thicker in depth but do not extend as much in the lateral direction. Area 4 shows low instantaneous frequencies at the eastern flank of the Gotland Deep. Low frequencies are visible within the well-stratified Quaternary layers as well as at the truncation of the Silurian successions against the base Quaternary. Area 5 depicts low instantaneous frequencies at distances between 0 and 18 km within the Lower Silurian right above the border to the Ordovician. Other areas of reduced instantaneous frequencies are also visible in other parts of the image, for example, scattered low frequencies within the area of the observed small-scale fractures in the Silurian succession (Figure 4a) or within the Quaternary deposits in the very southeast.

5. Interpretation and Discussion

5.1. Fluid Origin and Migration Paths

The seismic image in Figure 4a and the corresponding instantaneous frequency plot in Figure 7 contain several indications for the presence of fluids in the central Baltic Basin. Especially the blurred reflection below the base Devonian (Figure 4a), the low instantaneous frequencies at that location (area 2 in Figure 7) as well as the low instantaneous frequencies within the Lower Silurian, Devonian and Quaternary strata (areas 5, 3, and 1 in Figure 7) can be seen as indicators for fluids within the Silurian, Devonian and Quaternary successions (see also e.g., Abu El-Ata et al., 2019; Taner et al., 1979; Tai et al., 2009). Due to numerous oil accumulations and reservoirs as well as reports of oil seepage on the seabed in this region (De Vos et al., 2010; Johansson et al., 1943; Lapinskas, 2000; Pletsch et al., 2010; Schäfer et al., 2021; Sivhed et al., 2004; Wagner, 2011; Šliaupa & Hoth, 2011), it is a reasonable interpretation that these fluids are hydrocarbons. As biogenic fluids do not occur in the consolidated, originally deeply buried Silurian and Devonian strata, these hydrocarbons must be of thermogenic origin that migrated there from their source rocks. Within the Silurian and the Devonian, the hydrocarbons cluster below high amplitude reflections, suggesting that the corresponding reflectors represent at least some kind of barrier (Figures 4 and 7). Especially, the aggregation of low instantaneous frequencies below the dipped base Devonian horizon suggests that hydrocarbons migrate along the horizon in an updip direction toward the northwest. Such a migration could be driven by the buoyancy of the hydrocarbons. Similar fluid migration characteristics have previously been observed by Grob et al. (2020) in the Norwegian Trench. Given the known hydrocarbon reservoirs in the southeastern Baltic Basin (Figure 2) and the general structure of the basin with dipping layers toward the southeast (Figure 1b), we assume a general migration path from the southeast in an updip direction toward the northwest. The accumulation of hydrocarbons observed within the Lower Quaternary (area 1 in Figure 7) could therefore be sourced by such an updip migration system. A biogenic origin for these hydrocarbons seems unlikely, as it would require layers of organic-rich sediments. In the sub-bottom profiler data (Figures 5 and 6b) we do not observe any typical signs for those layers or shallow biogenic hydrocarbons, such as increased seismic blanking or reverberations.

Similar migration paths were also proposed by Sivhed et al. (2004) and Schäfer et al. (2021). The migration from the Cambrian and Ordovician source rocks toward the Silurian and Devonian layers—where we observe the hydrocarbons - can be facilitated through for example, small-scale fractures such as those observed within the Silurian strata in Figures 4a and 4c. Those fractures can cause pathways for fluids through thick successions, which are otherwise regarded as sealing layers. The vertical alignment of the diffraction energy at the locations of the layer distortions reinforces the interpretation of fractures and rules out other possible explanations for the layer mismatches such as different overburdens or velocity pull-ups or pull-downs. However, the high diffractivity overserved within the Quaternary succession is unrelated to these fractures and results from the rough surface of the base Quaternary related to erosion during the last glaciation.

The observed migration pathways along and across Paleozoic structures pose some potential challenges with respect to CCS, as they are illustrating that some reservoirs are leaking and that the fluids are able to migrate through the whole Paleozoic strata up to the seafloor. In addition, the observed pathways also demonstrate that seepage locations on the seafloor may not correlate to the locations of leaky reservoirs.

Although a thermogenic origin associated with the updip migration of fluids seems likely for most of the assumed hydrocarbon accumulations, the presence of biogenically related hydrocarbons cannot be ruled out completely. Especially within and at the flank of the Gotland Deep (area 4 in Figure 7), a biogenic origin is possible. While the hydrocarbons clustering below the base Quaternary are most likely of thermogenic origin related to the updip migration along dipping layers, this is not necessarily the case for the hydrocarbons within the Quaternary

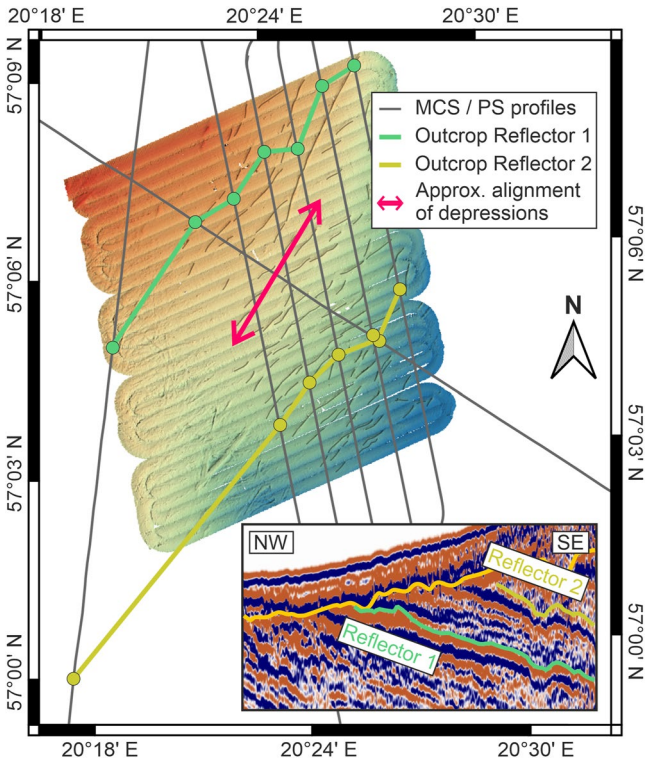

Figure 8. Lateral outcropping location of two Devonian reflectors in relation to the observed fluid escape structures (for location of the seismic image, see Figure 4a). MCS: Multi-Channel Seismic; PS: PARASOUND (sub-bottom profiler).

succession. These hydrocarbons seem to migrate within the Quaternary layer toward the flanks of the Gotland Deep on either side. The Quaternary layer is thicker than at the location of our multibeam survey and analyses from Christiansen et al. (2002) show an increased content of organic matter within shallow depths. This gives the potential for a biogenic origin of the hydrocarbons, which would be consistent with the assumptions from Endler (1998) that biogenic hydrocarbons exist in those areas as well. In contrast to Endler (1998), we also observed indications for hydrocarbons in the shallow sediments within the Gotland Deep, not only at its outer margins (Figure 7).

5.2. Fluid Escape Structures

The locations of the NE-SW oriented, elongated and channel-like depressions incising into the seafloor observed mostly in the central and eastern parts of the multibeam survey correlate well with the incisions into the post-glacial Holocene sediments observed in the sub-bottom profiler data (Figures 3 and 5). The shape of the incisions in the sub-bottom profiler images and the almost transparent areas below these structures as well as the spatial correlation to the observed hydrocarbon accumulation (area 1 in Figure 7) strongly suggest that they represent fluid related escape depressions (Cathles et al., 2010). This is also in agreement with findings from Endler (1998), who observed gas-charged sediments and individual pockmarks in sub-bottom profiler images at the shoulders of the Gotland Deep. As the sub-bottom profiler image that crosses the extraordinary long incision observed in the northeast of the multibeam survey does not show any significant differences to the scattered and smaller incisions in the central and eastern parts, we assume a fluid-flow related origin for this structure as well (Figures 5 and 6b).

The most common fluid escape structures are pockmarks, which typically are circular structures resulting from fluid discharge (see In Hovland & Judd, 1988; and references therein). In general, pockmarks are formed at locations where fluids escape upwards through fine-grained seafloor sediments. They can be linearly aligned along fault planes or paleochannels (Betzler et al., 2011; Sahling et al., 2008) but also be more randomly distributed (Forwick et al., 2009) or associated with salt diapirs (Sahling et al., 2008) or outcropping geological layers (Hübscher & Borowski, 2006). The expelling fluids may either be of biogenic (methane) or thermogenic (hydrocarbon) origin, whereby, in some cases, other forms of fluids such as freshwater or porewaters with small amounts of CO_2 and other gases have also been observed (Hovland & Judd, 1988; Hübscher & Borowski, 2006; Vogt et al., 1994). Elongated pockmarks are not as common as the typically known circular shape, but have been observed in several examples worldwide before (Bøe et al., 1998; Çifçi et al., 2003; Hovland et al., 2002; Hovland & Judd, 1988). Hovland et al. (2002) defined elongated pockmarks as depressions where one axis is much longer than the other axis. The length of these pockmarks is often reported as 1 km or less (Bøe et al., 1998; Hovland & Judd, 1988; León et al., 2010). Elongated pockmarks preferably occur on slopes and their morphogenesis is associated to bottom currents whose direction is approximately directed along the long axis of the pockmarks (Bøe et al., 1998; Hovland et al., 2002). However, the resulting morphology of current controlled pockmarks is rather elliptical than trench- or incision like. The elongation of the depressions we observed is mostly oriented in the NE-SW direction but varies between the individual depressions (Figures 3 and 8). This contradicts the idea of a bottom current origin, as then the alignment would be very similar for all elongated depressions (see, e.g., Figure 3 in Bøe et al. (1998)).

A second process that can lead to the formation of elongated pockmarks is the coalescence of several closely spaced individual pockmarks (Çifçi et al., 2003; Michel et al., 2017). However, as neither the multibeam nor the sub-bottom profiler data show any indications for the merger of two or more pockmarks such as described and shown by Çifçi et al. (2003), we also rule out this process for our study area.

Hence, other generic processes have to be considered for the formation of the elongated fluid escape structures. The orientations of the individual fluid escape depressions correlate with the general truncation trend of the

dipping Paleozoic layers against the base Quaternary unconformity (Figures 3 and 1b). Figure 8 maps the lateral outcropping location of two prominent Devonian horizons. Their exact location within the Devonian is illustrated in Figure 4a. The outcropping horizons are aligned in NE-SW direction, similar to the alignment of the observed scattered depressions, which is marked by the pink arrow in Figure 8. This spatial correlation of fluid escape structures and outcropping and fluid bearing Paleozoic layers strongly indicates a causal relation. This observation is consistent with the assumption that fluids assemble and escape at those locations where permeable strata terminate against the base Quaternary. The elongated form of the fluid escape structures could therefore be controlled by the location of the outcropping strata, which is driven either by tectonics or glacial erosion. The fluid escape is not limited to one location resulting in a circular structure but takes place along a larger area along the outcropping plane, thus, creating elongated escape structures. A similar tectonic setting where fluid escape is related to outcropping layers has previously been observed in the Skagerrak (Grob et al., 2020; Hübscher & Borowski, 2006).

If the elongated pockmarks are located above outcropping geologic strata, the fluids must migrate vertically upwards through the Quaternary sediments to the seafloor. Yet, as shown in Figure 5, pockmarks are more abundant than outcropping high-amplitude reflections, which should be considered as the main fluid source. Since the lateral resolution of the seismic data is much less than that of the PARASOUND data, it cannot be clearly determined whether the number of pockmarks is controlled by numerous fluid-bearing outcropping Paleozoic strata, or whether the fluids are further distributed as they pass through the overlying glacio-marine sediments. The shape of these sediments suggests that they were remobilized and slipped toward the Gotland Deep in the northwest (Figure 5). This could have led to NW-SE extension in the overlaying post glacial sediment layer, thus creating weakness zones supporting the formation of NE-SW oriented fluid pathways.

The fluid escape depressions shown in Figures 5 and 6b are not filled with sediments or the infill is thinner than 10–20 cm, which corresponds to the vertical resolution of the 4 kHz PARASOUND signal (wavelength approx. 40 cm). This can either indicate recent or ongoing fluid escape activity or be a result of strong bottom currents which prevent sedimentation. As sediments are present adjacent to the depressions, the presence of strong sedimentation hampering bottom currents is unlikely, therefore, it is assumed that these structures are currently active. If this is an episodic, quasi-episodic or continuous process cannot be assessed in this study. In previous studies in various different study areas around the world, both processes have been observed (e.g., Betzler et al., 2011; Bøe et al., 1998; Çifçi et al., 2003; Gay et al., 2003; Sahling et al., 2008).

5.3. Glacially Related Processes

The sub-bottom profiler image crossing the more chaotic structures in the west and southwest of the mapped bathymetry shows fundamental differences to the sub-bottom profiler images crossing the elongated fluid escape depressions described in Section 5.2 (Figures 5 and 6a and 6b). The irregular, rough and scraped-like seafloor is comparable to an area observed in the seismic image in Figure 4a. There, at distances between 50 and 55 km, the otherwise smooth seafloor is interrupted by several peaks pinching out of the seafloor. These characteristics are comparable to observations from Dowdeswell et al. (1997), Karpin et al. (2021), and Lehmann et al. (2022), who related such structures to icebergs scours. Those scours are formed when icebergs with keel depths exceeding the water depth incise into the seafloor. Driven by wind force and ocean currents, the icebergs plough through the seafloor sediments producing distinctive linear/curvilinear marks (Dorokhov et al., 2018). During the last deglaciation about 10,000 to 12,000 years ago, the sea level in the central Baltic Sea was several tens of meters higher than today's sea level (Karpin et al., 2021; Rosentau et al., 2021). As iceberg scours have been reported in water depths exceeding 500 m, it is nonetheless possible that iceberg scouring is responsible for the observed structures (Dowdeswell et al., 1992). Similar structures have also been observed at the outer slope of the Klints Bank and within the Gotland depression southwest of our study area (Dorokhov et al., 2018; Endler, 1998). However, Endler (1998) suggested that a relation of such scour marks to erosional processes during the last deglaciation is more likely. This assumption was challenged by Dorokhov et al. (2018), who ruled out erosional processes and determined icebergs as cause for the observed incisions. They argued that the size and chaotic orientation are incompatible with erosional processes. Due to the chaotic orientation and the vicinity of our observed structures to the ones from Dorokhov et al. (2018), we also regard iceberg scours as the most likely cause for most of the observed structures. However, for the larger channel-like structures marked with black arrows in Figure 3, an erosional origin remains a likely explanation as these structures are too large for iceberg scour marks. Other

explanations such as marks from fishing gear can be disregarded as they penetrate the seafloor only up to several tens of centimeters, which is far less than the incision depths of several meters we observed for our structures (Eigaard et al., 2016).

In addition to the prominent iceberg scours at the seafloor, Figures 6a and 6b also exhibit a rough and irregular surface of the glacial till deposits in areas where they are overlain by glacio-marine and post-glacial sediments. Especially several features in the northeast of Figure 6a and the incision at a distance of approximately 2 km in Figure 6b show similar characteristics as the iceberg scours. Consequently, those structures could represent buried iceberg scours that were filled during later sedimentation. Comparable structures have previously been described in the Baltic Sea by Karpin et al. (2021). Hovland and Judd (1988) suggested a relation between iceberg scours and pockmarks. They noted that pockmarks have been observed in the vicinity of iceberg scours with far greater abundance than elsewhere and suggested that iceberg scouring may induce stress into the shallow sediments creating small-scale fractures and fissures and therefore facilitating local fluid escape. Additionally, they proposed that the formation of pockmarks near buried iceberg scours is supported by soft sediments infilling the scours.

6. Conclusion

Based on our analysis of a combination of 2D seismic, sediment sub-bottom profiler and multibeam echosounder data from the central Baltic Basin, we identified a field of several individual fluid escape depressions at the eastern margin of the Gotland Deep and revealed insights into the fluid migration system sourcing these structures. For the first time, we are able to show evidence for the migration paths from the Silurian and Devonian strata up to the seafloor. Additionally, we imaged scraped-like structures covering the seafloor that we interpret as iceberg scours resulting from the last deglaciation.

Our results show that hydrocarbons migrate within the Baltic Basin in an updip direction beneath sealing Paleozoic reflectors from the southeast toward the northwest. The source of these hydrocarbons could not be imaged. However, based on previous studies we assume the source rocks to be located in the southeastern Baltic Basin (e.g., Liepaja-Saldus Ridge). Advanced diffraction imaging allowed us to clearly identify small-scale fractures within the Silurian strata, which we assume facilitate upwards migration of hydrocarbons through otherwise sealing reflectors. At locations, where truncated dipping Paleozoic reflectors terminate against the base Quaternary, the hydrocarbons escape through elongated fluid escape depressions that we observed at the seafloor. The locations of these depressions and their elongated shapes are directly controlled by the regional geologic setting of our study area and thus exhibit a different genesis mechanism than elongated pockmarks formed through bottom currents or the coalescence of several individual pockmarks. With a length of more than 5 km, we also observed one of the largest elongated fluid related escape depression that has been described in literature so far. The migration of the fluids through the Quaternary deposits may have been influenced by the effects of iceberg scouring, which are known to facilitate local fluid escape and which we have observed in the vicinity of the pockmarks.

In addition to the thermogenic fluids associated to the described migration system, we also observed fluids within the Gotland Deep whose origin is more ambiguous. A biogenic origin for these fluids within the Quaternary succession cannot be ruled out, however, further biogeochemical analysis and sampling is required for a clear determination and to fully unravel the different hydrocarbon origins.

Our observations demonstrate that at least some Paleozoic hydrocarbon reservoirs in the southeastern Baltic Basin must be leaking and thus sourcing the migration pathways we described. With respect to potential CCS in this area, this represents a challenge that needs careful investigation. This study also shows that the effects of leaking reservoirs will not occur at the location of the reservoirs but depending the regional geological structure might be observable in far greater distances. This study also proves that the diffraction imaging technique is a useful tool for the identification of small-scale faults and possible leakage pathways along fault planes.

Data Availability Statement

The seismic data (Warwel et al., 2023a), sub-bottom echosounder data (Warwel et al., 2023c) and multibeam echosounder data (Warwel et al., 2023b) included in this manuscript are available in the PANGEA database.

Acknowledgments
We like to thank captain Rainer Hammacher and his entire crew of RV METEOR for their support during our M177 measurement campaign. The ship time and funding for initial data analysis was provided by the German Research Foundation (DFG; M177). We gratefully acknowledge Schlumberger for providing the 2021 VISTA SEISMIC DATA PROCESSING and the 2021 PETREL software as well as IHS Markit for providing the KINGDOM seismic interpretation software. QPS is thanked for providing the QPS QIMERA software. Open Access funding enabled and organized by Projekt DEAL.

References

Abu El-Ata, A. S., El-Behiry, M. G., & Hussein, M. (2019). Applications of the frequency analysis, using the spectral decomposition in the reservoir characterization. *Geomechanics and Geophysics for Geo-Energy and Geo-Resources*, *5*(4), 457–478. https://doi.org/10.1007/s40948-019-00118-z

Ahlrichs, N., Hübscher, C., Andersen, T. R., Preine, J., Bogner, L., & Schäfer, W. (2023). The Langeland Fault System unravelled: Quaternary fault reactivation along an elevated basement block between the North German and Norwegian–Danish basins. *Boreas*. https://doi.org/10.1111/bor.12614

Andrén, T., Björck, S., Andrén, E., Conley, D., Zillén, L., & Anjar, J. (2011). The development of the Baltic Sea Basin during the last 130 ka. In J. Harff, S. Björck, & P. Hoth (Eds.), *The Baltic Sea Basin. Central and Eastern European Development Studies (CEEDES)* (pp. 75–97). Springer. https://doi.org/10.1007/978-3-642-17220-5_4

Betzler, C., Lindhorst, S., Hübscher, C., Lüdmann, T., Fürstenau, J., & Reijmer, J. (2011). Giant pockmarks in a carbonate platform (Maldives, Indian Ocean). *Marine Geology*, *289*(1–4), 1–16. https://doi.org/10.1016/j.margeo.2011.09.004

Bøe, R., Rise, L., & Ottesen, D. (1998). Elongate depressions on the southern slope of the Norwegian Trench (Skagerrak): Morphology and evolution. *Marine Geology*, *146*(1–4), 191–203. https://doi.org/10.1016/S0025-3227(97)00133-3

Brangulis, A. P., Kanev, S. V., Margulis, L. S., & Haselton, T. M. (1992). Hydrocarbon geology of the Baltic Republics and the adjacent Baltic Sea. In A. M. Spencer (Ed.), *Generation, accumulation and production of Europe's hydrocarbons* (Vol. 2, pp. 111–115). Special Publication of the European Association of Petroleum Geoscientists.

Cathles, L. M., Su, Z., & Chen, D. (2010). The physics of gas chimney and pockmark formation, with implications for assessment of seafloor hazards and gas sequestration. *Marine and Petroleum Geology*, *27*(1), 82–91. https://doi.org/10.1016/j.marpetgeo.2009.09.010

Christiansen, C., Kunzendorf, H., Emeis, K. C., Endler, R., Struck, U., Neumann, T., & Sivkov, V. (2002). Temporal and spatial sedimentation rate variabilities in the eastern Gotland Basin, the Baltic Sea. *Boreas*, *31*(1), 65–74. https://doi.org/10.1111/j.1502-3885.2002.tb01056.x

Çifçi, G., Dondurur, D., & Ergün, M. (2003). Deep and shallow structures of large pockmarks in the Turkish shelf, Eastern Black Sea. *Geo-Marine Letters*, *23*(3), 311–322. https://doi.org/10.1007/s00367-003-0138-x

De Vos, W., Feldrappe, H., Pharaoh, T. C., Smith, N. J. P., Vejbæk, O. V., Verniers, J., et al. (2010). Pre-devonian. In J. C. Doornenbal & A. G. Stevenson (Eds.), *Petroleum geological Atlas of the Southern Permian Basin Area* (pp. 59–69). EAGE Publications.

Dewar, M., Wei, W., McNeil, D., & Chen, B. (2013). Small-scale modelling of the physiochemical impacts of CO2 leaked from sub-seabed reservoirs or pipelines within the North Sea and surrounding waters. *Marine Pollution Bulletin*, *73*(2), 504–515. https://doi.org/10.1016/j.marpolbul.2013.03.005

Dobrova, H., Kolly, E., & Schmitz, U. (2003). E and P ventures in the Eastern-Central Europe transformation states after 1989 - A review of expectations and results. *Oil Gas: European Magazine*, *29*(4), 172–212.

Dorokhov, D. V., Dorokhova, E. V., & Sivkov, V. V. (2018). Iceberg and ice-keel ploughmarks on the Gdansk-Gotland Sill (south-eastern Baltic Sea). *Geo-Marine Letters*, *38*(1), 83–94. https://doi.org/10.1007/s00367-017-0517-3

Dowdeswell, J. A., Whittington, R. J., & Hodgkins, R. (1992). The sizes, frequencies, and freeboards of East Greenland icebergs observed using ship radar and sextant. *Journal of Geophysical Research*, *97*(C3), 3515–3528. https://doi.org/10.1029/91JC02821

Dowdeswell, J. A., Whittington, R. J., & Villinger, H. (1997). Iceberg scours: Records from broad and narrow-beam acoustic systems. In T. A. Davies, T. Bell, A. Cooper, H. Josenhans, L. Polyak, A. Solheim, et al. (Eds.), *Glaciated continental margins – An Atlas of acoustic images* (pp. 27–28). Springer.

Ehlers, J., Grube, A., Stephan, H. J., & Wansa, S. (2011). Pleistocene glaciations of North Germany - New results. In J. Ehlers, P. L. Gibbard, & P. D. Hughes (Eds.), *Developments in quaternary sciences* (pp. 149–162). Elsevier. https://doi.org/10.1016/B978-0-444-53447-7.00013-1

Eigaard, O. R., Bastardie, F., Breen, M., Dinesen, G. E., Hintzen, N. T., Laffargue, P., et al. (2016). Estimating seabed pressure from demersal trawls, seines, and dredges based on gear design and dimensions. *ICES Journal of Marine Science*, *73*(suppl_1), i27–i43. https://doi.org/10.1093/icesjms/fsv099

EMODnet Bathymetry Consortium. (2020). *EMODnet Digital Bathymetry (DTM)*. https://doi.org/10.12770/bb6a87dd-e579-4036-abe1-e649cea9881a

Endler, R. (1998). Acoustic studies. In K.-C. Emeis & U. Struck (Eds.), *Gotland Basin Experiment (GOBEX) - status report on investigations concerning Benthic processes, sediment formation and accumulation* (Vol. 34, pp. 21–34). Marine Science Reports.

Flodén, T., Bjerkéus, M., Tuuling, I., & Eriksson, M. (2001). A Silurian reefal succession in the Gotland area, Baltic Sea. *GFF*, *123*(3), 137–152. https://doi.org/10.1080/11035890101233137

Ford, J., Urgeles, R., Camerlenghi, A., & Gràcia, E. (2021). Seismic diffraction imaging to characterize mass-transport complexes: Examples from the Gulf of Cadiz, south west Iberian margin. *Journal of Geophysical Research: Solid Earth*, *126*(3), e2020JB021474. https://doi.org/10.1029/2020JB021474

Forwick, M., Baeten, N. J., & Vorren, T. O. (2009). Pockmarks in Spitsbergen fjords. *Norwegian Journal of Geology/Norsk Geologisk Forening*, *89*, 65–77.

Gay, A., Lopez, M., Cochonat, P., Sultan, N., Cauquil, E., & Brigaud, F. (2003). Sinuous pockmark belt as indicator of a shallow buried turbiditic channel on the lower slope of the Congo Basin, West African Margin. *Geological Society, London, Special Publications*, *216*(1), 173–189. https://doi.org/10.1144/GSL.SP.2003.216.01.12

Gelumbauskaitė, L. Ž. (1995). Bottom relief and Genesis of the Gotland depression. *Baltica*, *9*, 65–75.

Grad, M., & Polkowski, M. (2016). Seismic basement in Poland. *International Journal of Earth Sciences*, *105*(4), 1199–1214. https://doi.org/10.1007/s00531-015-1233-8

Grob, H., Seidel, E., & Hübscher, C. (2020). Seismic amplitude and attribute data from Mesozoic strata in the Skagerrak (Danish-Norwegian North Sea): Indicators for fluid migration and seal bypass systems. *Marine and Petroleum Geology*, *121*, 104596. https://doi.org/10.1016/j.marpetgeo.2020.104596

Hall, A., & van Boeckel, M. (2020). Origin of the Baltic Sea basin by Pleistocene glacial erosion. *GFF*, *142*(3), 237–252. https://doi.org/10.1080/11035897.2020.1781246

Heggland, R. (1998). Gas seepage as an indicator of deeper prospective reservoirs. A study based on exploration 3D seismic data. *Marine and Petroleum Geology*, *15*(1), 1–9. https://doi.org/10.1016/S0264-8172(97)00060-3

Houmark-Nielsen, M. (2011). Pleistocene glaciations in Denmark: A closer look at chronology, ice dynamics and landforms. In J. Ehlers, P. L. Gibbard, & P. D. Hughes (Eds.), *Developments in quaternary sciences* (pp. 47–58). Elsevier. https://doi.org/10.1016/B978-0-444-53447-7.00005-2

Hovland, M., Gardner, J. V., & Judd, A. G. (2002). The significance of pockmarks to understanding fluid flow processes and geohazards. *Geofluids*, *2*(2), 127–136. https://doi.org/10.1046/j.1468-8123.2002.00028.x

Hovland, M. & Judd, A. G. (Eds.) (1988). *Seabed pockmarks and seepages: Impact on geology, biology and the marine environment*. Graham and Trotman Limited.

Hübscher, C., Artschwager, M., Aster, M., Barbosa, I., Bogner, L., Häcker, T., et al. (2022). Geophysical investigation of the Paleozoic basement in the Gotland depression and its margins: Tectonics and reefs, hydrocarbon fluid escape and CO_2 storage potential, cruise No. M177, October 22 - November 18, 2021, Emden (Germany) - Emden (Germany). *METEOR-Berichte*, *M177*, 1–38. https://doi.org/10.48433/cr_m177

Hübscher, C., & Borowski, C. (2006). Seismic evidence for fluid escape from Mesozoic cuesta type topography in the Skagerrak. *Marine and Petroleum Geology*, *23*(1), 17–28. https://doi.org/10.1016/j.marpetgeo.2005.07.004

Huuse, M., & Lykke-Andersen, H. (2000). Overdeepened Quaternary valleys in the eastern Danish north sea: Morphology and origin. *Quaternary Science Reviews*, *19*(12), 1233–1253. https://doi.org/10.1016/S0277-3791(99)00103-1

Johansson, S., Sundius, N. G., & Westergård, A. H. (1943). *Beskrivning till kartbladet Lidköping*. Kungl. boktryckeriet, PA Norstedt & söner. (in Swedish).

Judd, A. G. (2003). The global importance and context of methane escape from the seabed. *Geo-Marine Letters*, *23*(3), 147–154. https://doi.org/10.1007/s00367-003-0136-z

Judd, A. G. & Hovland, M. (Eds.) (2009)., *Seabed fluid flow: The impact on geology, biology and the marine environment*. Cambridge University Press.

Kanev, S., Margulis, L., Bojesen-Koefoed, J. A., Weil, W. A., Merta, H., & Zdanaviciute, O. (1994). Oils and hydrocarbon source rocks of the Baltic syneclise. *Oil & Gas Journal*, *92*(28).

Karpin, V., Heinsalu, A., & Virtasalo, J. J. (2021). Late Pleistocene iceberg scouring in the north-eastern Baltic Sea, west of Estonia. *Marine Geology*, *438*, 106537. https://doi.org/10.1016/j.margeo.2021.106537

Kearey, P., Brooks, M., & Hill, I. (Eds.) (2002). *An introduction to geophysical exploration* (Vol. 4). John Wiley & Sons.

Landa, E., & Keydar, S. (1998). Seismic monitoring of diffraction images for detection of local heterogeneities. *Geophysics*, *63*(3), 1093–1100. https://doi.org/10.1190/1.1444387

Lapinskas, P. (2000). *Structure and petroliferosity of the Silurian in Lithuania* (p. 203). Institute of Geology.

Lehmann, C., Jokat, W., & Coakley, B. (2022). Glacial sediments on the outer Chukchi Shelf and Chukchi Borderland in seismic reflection data. *Marine Geophysical Researches*, *43*(3), 1–16. https://doi.org/10.1007/s11001-022-09497-7

León, R., Somoza, L., Medialdea, T., Hernández-Molina, F. J., Vázquez, J. T., Díaz-del-Rio, V., & González, F. J. (2010). Pockmarks, collapses and blind valleys in the Gulf of Cádiz. *Geo-Marine Letters*, *30*(3), 231–247. https://doi.org/10.1007/s00367-009-0169-z

Licht, K. (2009). Glaciomarine sediments. In V. Gornitz (Ed.), *Encyclopedia of paleoclimatology and ancient environments. Encyclopedia of Earth sciences series* (pp. 395–396). Springer. https://doi.org/10.1007/978-1-4020-4411-3_99

Lidmar-Bergström, K., & Olvmo, M. (2015). *Plains, steps, Hilly Relief and valleys in northern Sweden - review, interpretations and implications for conclusions on phanerozoic tectonics*. Sveriges geologiska undersökning.

MacDonald, I. R., Leifer, I., Sassen, R., Stine, P., Mitchell, R., & Guinasso, N., Jr. (2002). Transfer of hydrocarbons from natural seeps to the water column and atmosphere. *Geofluids*, *2*(2), 95–107. https://doi.org/10.1046/j.1468-8123.2002.00023.x

Mazur, S., Mikolajczak, M., Krzywiec, P., Malinowski, M., Buffenmyer, V., & Lewandowski, M. (2015). Is the Teisseyre-Tornquist zone an ancient plate boundary of Baltica? *Tectonics*, *34*(12), 2465–2477. https://doi.org/10.1002/2015TC003934

Michel, G., Dupré, S., Baltzer, A., Ehrhold, A., Imbert, P., Pitel, M., et al. (2017). Pockmarks on the South Aquitaine Margin continental slope: The seabed expression of past fluid circulation and former bottom currents. *Comptes Rendus Geoscience*, *349*(8), 391–401. https://doi.org/10.1016/j.crte.2017.10.003

Mityagina, M., & Lavrova, O. (2016). Satellite survey of inner seas: Oil pollution in the black and Caspian seas. *Remote Sensing*, *8*(10), 875. https://doi.org/10.3390/rs8100875

O'Neill, N., Pasquali, R., Vernon, R., & Niemi, A. (2014). Geological storage of CO2 in the southern Baltic Sea. *Energy Procedia*, *59*, 433–439. https://doi.org/10.1016/j.egypro.2014.10.399

Pletsch, T., Appel, J., Botor, D., Clayton, C. J., Duin, E. J. T., Faber, E., et al. (2010). Petroleum generation and migration. In J. C. Doornenbal & A. G. Stevenson (Eds.), *Petroleum Geological Atlas of the Southern Permian Basin Area* (pp. 225–253). EAGE Publications.

Poprawa, P., Šliaupa, S., Stephenson, R., & Lazauskien, J. (1999). Late Vendian - Early Palaeozoic tectonic evolution of the Baltic Basin: Regional tectonic implications from subsidence analysis. *Tectonophysics*, *314*(1–3), 219–239. https://doi.org/10.1016/S0040-1951(99)00245-0

Preine, J., Schwarz, B., Bauer, A., & Hübscher, C. (2020). When there is No offset: A demonstration of seismic diffraction imaging and depth-velocity Model Building in the Southern Aegean Sea. *Journal of Geophysical Research: Solid Earth*, *125*(9), e2020JB019961. https://doi.org/10.1029/2020JB019961

Römer, M., Blumenberg, M., Heeschen, K., Schloemer, S., Müller, H., Müller, S., et al. (2021). Seafloor methane seepage related to salt diapirism in the northwestern part of the German North Sea. *Frontiers of Earth Science*, *9*, 556329. https://doi.org/10.3389/feart.2021.556329

Rosentau, A., Klemann, V., Bennike, O., Steffen, H., Wehr, J., Latinović, M., et al. (2021). A Holocene relative sea-level database for the Baltic Sea. *Quaternary Science Reviews*, *266*, 107071. https://doi.org/10.1016/j.quascirev.2021.107071

Sahling, H., Bohrmann, G., Spiess, V., Bialas, J., Breitzke, M., Ivanov, M., et al. (2008). Pockmarks in the Northern Congo Fan area, SW Africa: Complex seafloor features shaped by fluid flow. *Marine Geology*, *249*(3–4), 206–225. https://doi.org/10.1016/j.margeo.2007.11.010

Schäfer, W., Hübscher, C., & Sopher, D. (2021). Seismic stratigraphy of the Klints Bank east of Gotland (Baltic Sea): A giant drumlin sealing thermogenic hydrocarbons. *Geo-Marine Letters*, *41*(1), 1–15. https://doi.org/10.1007/s00367-020-00683-3

Schwarz, B. (2019a). Chapter One - An introduction to seismic diffraction. In C. Schmelzbach (Ed.), *Advances in Geophysics* (pp. 1–64). Elsevier. https://doi.org/10.1016/bs.agph.2019.05.001

Schwarz, B. (2019b). Coherent wavefield subtraction for diffraction separation. *Geophysics*, *84*(3), V157–V168. https://doi.org/10.1190/geo2018-0368.1

Schwarz, B., & Gajewski, D. (2017). Accessing the diffracted wavefield by coherent subtraction. *Geophysical Journal International*, *211*(1), 45–49. https://doi.org/10.1093/gji/ggx291

Schwarz, B., & Krawczyk, C. M. (2020). Coherent diffraction imaging for enhanced fault and fracture network characterization. *Solid Earth*, *11*(5), 1891–1907. https://doi.org/10.5194/se-11-1891-2020

Shogenov, K., Shogenova, A., Gei, D., & Forlin, E. (2017). Synergy of CO_2 storage and oil recovery in different geological formations: Case study in the Baltic Sea. *Energy Procedia*, *114*, 7047–7054. https://doi.org/10.1016/j.egypro.2017.03.1846

Shogenova, A., Šliaupa, S., Vaher, R., Shogenov, K., & Pomeranceva, R. (2009). The Baltic Basin: Structure, properties of reservoir rocks, and capacity for geological storage of CO_2. *Estonian Journal of Earth Sciences*, *58*(4), 259–267. https://doi.org/10.3176/earth.2009.4.04

Sivhed, U., Erlström, M., Bojesen-Koefoed, J. A., & Löfgren, A. (2004). Upper Ordovician carbonate mounds on Gotland, central Baltic Sea: Distribution, composition and reservoir characteristics. *Journal of Petroleum Geology*, *27*(2), 115–140. https://doi.org/10.1111/j.1747-5457.2004.tb00049.x

Šliaupa, S. (1999). Far-field stress transmission indications in Early Palaeozoic structural evolution of the Baltic basin. *Romanian Journal of Tectonics and Regional Geology*, *77*(1), 59.

Šliaupa, S., Fokin, P., Lazauskiene, J., & Stephenson, R. A. (2006). The Vendian - Early Palaeozoic sedimentary basins of the East European Craton. In D. G. Gee & R. A. Stephenson (Eds.), *European lithosphere dynamics* (Vol. 32, pp. 449–462). Geological Society. https://doi.org/10.1144/GSL.MEM.2006.032.01.28

Šliaupa, S., & Hoth, P. (2011). Geological evolution and Resources of the Baltic Sea area from the Precambrian to the Quaternary. In J. Harff, S. Björck, & P. Hoth (Eds.), *The Baltic Sea Basin. Central and Eastern European Development Studies (CEEDES)* (pp. 13–51). Springer. https://doi.org/10.1007/978-3-642-17220-5_2

Šliaupa, S., Laškovas, E., Lazauskienė, J., Laškova, L., & Sidorov, V. (2004). The petroleum system of the Lithuanian offshore region. *Zeitschrift für Angewandte Geology. Hannover*, 41–59.

SLR Report. (2014). Final report on prospective sites for the geological storage of CO_2 in the southern Baltic Sea. SLR Ref.: 501-00302-00001. Retrieved from https://www.globalccsinstitute.com/resources/publications-reports-research/final-report-on-prospective-sites-for-the-geological-storage-of-co2-in-the-southern-baltic-sea

Sopher, D., Erlström, M., Bell, N., & Juhlin, C. (2016). The structure and stratigraphy of the sedimentary succession in the Swedish sector of the Baltic Basin: New insights from vintage 2D marine seismic data. *Tectonophysics*, *676*, 90–111. https://doi.org/10.1016/j.tecto.2016.03.012

Sopher, D., Juhlin, C., & Erlström, M. (2014). A probabilistic assessment of the effective CO_2 storage capacity within the Swedish sector of the Baltic Basin. *International Journal of Greenhouse Gas Control*, *30*, 148–170. https://doi.org/10.1016/j.ijggc.2014.09.009

Tai, S., Puryear, C., & Castagna, J. P. (2009). *Local frequency as a direct hydrocarbon indicator*. SEG Technical Program Expanded Abstracts. https://doi.org/10.1190/1.3255284

Taner, M. T., Koehler, F., & Sheriff, R. E. (1979). Complex seismic trace analysis. *Geophysics*, *44*(6), 1041–1063. https://doi.org/10.1190/1.1440994

Tarkowski, R. (2017). Perspectives of using the geological subsurface for hydrogen storage in Poland. *International Journal of Hydrogen Energy*, *42*(1), 347–355. https://doi.org/10.1016/j.ijhydene.2016.10.136

Tuuling, I. (2019). The Leba Ridge–Riga–Pskov Fault Zone–a major East European Craton interior dislocation zone and its role in the early Palaeozoic development of the platform cover. *Estonian Journal of Earth Sciences*, *68*(4), 161–189. https://doi.org/10.3176/earth.2019.12

Tuuling, I., Bauert, H., Willman, S., & Budd, G. (Eds.) (2011). *The Baltic Sea: Geology and Geotourism highlights* (1st ed.). NGO GEOGuide Baltoscandia.

Ūsaityt, D. (2000). The geology of the southeastern Baltic Sea: A review. *Earth-Science Reviews*, *50*(3–4), 137–225. https://doi.org/10.1016/S0012-8252(00)00002-7

Verschuur, D. J., Berkhout, A. J., & Wapenaar, C. P. A. (1992). Adaptive surface-related multiple elimination. *Geophysics*, *57*(9), 1166–1177. https://doi.org/10.1190/1.1443330

Vogt, P. R., Crane, K., Sundvor, E., Max, M. D., & Pfirman, S. L. (1994). Methane-generated (?) pockmarks on young, thickly sedimented oceanic crust in the Arctic: Vestnesa ridge, Fram strait. *Geology*, *22*(3), 255–258. https://doi.org/10.1130/0091-7613(1994)022<0255:MGPOYT>2.3.CO;2

Wagner, R. (2011). Natural migration of liquid and gaseous subsurface hydrocarbons into bottom sediments and waters. In S. Uścinowicz (Ed.), *Geochemistry of Baltic Sea surface sediments* (pp. 125–145). Polish Geological Institute - National Research Institute.

Warwel, A., Hübscher, C., Hartge, M., Artschwager, M., Schäfer, W., Preine, J., et al. (2023a). 2D multichannel seismic reflection processed data (GI Gun working area dataset) of RV METEOR during cruise M177, Gotland Basin, Baltic Sea [Dataset]. PANGAEA. https://doi.org/10.1594/PANGAEA.957436

Warwel, A., Hübscher, C., Hartge, M., Artschwager, M., Schäfer, W., Preine, J., et al. (2023b). Multibeam bathymetry processed data (Kongsberg EM710 working area dataset) of RV METEOR during cruise M177, Gotland Basin, Baltic Sea. [Dataset]. PANGAEA. https://doi.org/10.1594/PANGAEA.956740

Warwel, A., Hübscher, C., Hartge, M., Artschwager, M., Schäfer, W., Preine, J., et al. (2023c). Sediment echosounder processed data (Atlas Parasound P70 working area dataset) of RV METEOR during cruise M177, Gotland Basin, Baltic Sea. [Dataset]. PANGAEA. https://doi.org/10.1594/PANGAEA.957422

Winterhalter, B. (2001). On sediment Patchiness at the BASYS coring site, Gotland Deep, Baltic Sea. *Baltica*, *14*, 18–23.

Woźniak, P. P., & Czubla, P. (2015). The late Weichselian glacial record in northern Poland: A new look at debris transport routes by the Fennoscandian ice sheet. *Quaternary International*, *386*, 3–17. https://doi.org/10.1016/j.quaint.2015.01.014

Yilmaz, Ö. (Ed.) (2001). *Seismic data analysis: Processing, inversion, and interpretation of seismic data*. Society of Exploration Geophysicists.

Zdanaviciute, O., & Lazauskiene, J. (2004). Hydrocarbon migration and entrapment in the Baltic syneclise. *Organic Geochemistry*, *35*(4), 517–527. https://doi.org/10.1016/j.orggeochem.2004.01.016

Zecchin, M., & Rebesco, M. (2018). Glacigenic and glacimarine sedimentation from shelf to trough settings in the NW Barents Sea. *Marine Geology*, *402*, 184–193. https://doi.org/10.1016/j.margeo.2018.02.014

Ziegler, P. A. (Ed.) (1990)., *Geological Atlas of Western and Central Europe* (2nd ed.). Shell International Petroleum Maatschappij BV, distributed by Geological Society Publishing House, London.